Superconductor–Insulator Transition in NbTiN Films

M. V. Burdastyh[a, b], S. V. Postolova[a, b], T. I. Baturina[a, b], T. Proslier[c, d], V. M. Vinokur[d, e], and A. Yu. Mironov[a, b, *]

[a] *Rzhanov Institute of Semiconductor Physics, Siberian Branch, Russian Academy of Sciences, Novosibirsk, 630090 Russia*

[b] *Novosibirsk State University, Novosibirsk, 630090 Russia*

[c] *Institut de recherches sur les lois fundamentales de l'univers, Commissariat de l'énergie atomique et aux énergies renouvelables-Saclay, 91191 Gif-sur-Yvette, France*

[d] *Materials Science Division, Argonne National Laboratory, Argonne, IL 60439, USA*

[e] *Computation Institute, University of Chicago, Chicago, IL 60637, USA*

**e-mail: mironov@isp.nsc.ru*

Experimental results indicating a direct disorder-induced superconductor–insulator transition in NbTiN thin films have been reported. It has been shown that an increase in the resistance per square in the normal state is accompanied by the suppression of the critical temperature of the superconducting transition T_c according to the fermion mechanism of suppression of superconductivity by disorder. At the same time, the temperature of the Berezinskii–Kosterlitz–Thouless transition is completely suppressed at a nonzero critical temperature and, then, the ground state changes to insulating, which is characteristic of the boson model of suppression of superconductivity by disorder. It has been shown that the temperature dependences of the resistance of insulating films follow the Arrhenius activation law.

A superconductor–insulator transition (SIT) in thin disordered films has been studied theoretically and experimentally for several decades [1–3]. The suppression of the critical temperature of the superconducting transition T_c when approaching the SIT is a characteristic feature of this transition. In view of this circumstance, its study began with the observation of the suppression of the critical transition temperature at a decrease in the thickness of the sample [1]. The next studies showed that the best correlation appears not between T_c and the thickness of the film but between T_c and the resistance of a square segment of the film $R_\square$, the so-called resistance per square [4]. More recently, the suppression of T_c at an increase in the resistance of the film in the normal state was described at a microscopic level in [5]. At present, there are two main scenarios explaining a quantum transition from the superconducting state to an insulating one. In the first, fermion scenario [5], Cooper pairs are destroyed and normal electrons are localized in a nonsuperconducting state. In the second, boson scenario [6, 7], Cooper pairs are localized but continue to exist in an insulating state. Thus, in the case of the fermion scenario, the transition from a superconducting to an insulating state occurs in two stages: as the resistance per square in the normal state $R_\square$ increases, a superconductor–metal transition occurs first because of the complete disappearance of Cooper pairs, metallic states are then observed in a wide range of $R_\square$, and a metal–insulator transition finally occurs. In the boson scenario, the transition from a superconducting to an insulating phase occurs through a metallic state, which is implemented at a single point at the resistance R_c [7]. In the conventional superconductors, the superconductor–metal–insulator transition is usually observed in germanides and silicides of various compounds [8–10], and the direct superconductor–insulator transition with increasing $R_\square$ in the normal state, i.e., with increasing disorder, was detected in InO_x [11–13], Be [14], and TiN [15] films. At the same time, the resistance R_c in the cited experiments, in contrast to early expectations, was not universal and equal to the resistance quantum $h/4e^2 = 6.45$ kΩ/□. At present, there are several theoretical models of the forming of the insulating phase with increasing disorder [6, 7, 16, 17] and a particular mechanism of the direct superconductor–insulator transition is still unclear.

In this work, the disorder-induced superconductor–insulator transition in $Nb_{0.67}Ti_{0.33}N$ films is experimentally studied. This compound is of fundamental interest because its crystal lattice corresponds to the lattice of niobium nitride NbN where 33% of niobium atoms are replaced by titanium atoms. Pure NbN films

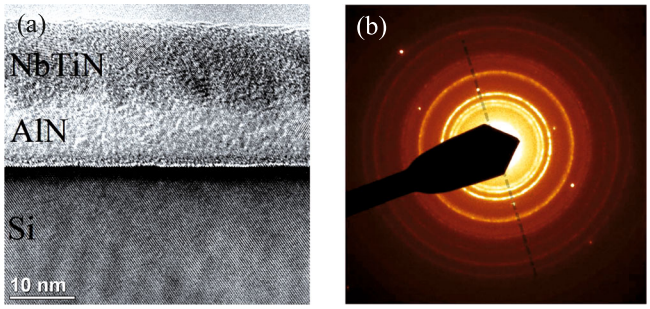

Fig. 1. (Color online) (a) Image of the cross section in a high-resolution transmission electron microscope. (b) Diffraction pattern.

have excellent superconducting properties (T_c up to 20 K and the upper critical field $B_{c2}(0)$ up to 20 T [18, 19]), whereas the T_c and $B_{c2}(0)$ values of TiN films are several times lower. With increasing disorder, the superconductor–metal–insulator transition occurs in NbN films and the direct superconductor–insulator transition occurs in TiN films [20]. Thus, the substitution of Nb atoms for Ti atoms in TiN makes it possible to enhance the superconducting properties of the film and to change the characteristic parameters of the superconductor–insulator transition.

We studied a set of NbTiN films grown by the atomic layer deposition method at a temperature of 350°C. The prepared films had a thickness of $d = 9$–18 nm. The degree of disorder was characterized by the resistance at liquid nitrogen temperature R_{77} varying from 0.7 to 4.6 kΩ. To obtain films thinner than 9 nm, we used the plasmochemical etching procedure for up to 7 s. The temperature dependences of the resistance were measured for 50-μm-wide Hall bar samples fabricated by the photolithography method. The distance between the potentiometric contacts was 450 μm and the distance between the current contacts was 2.5 mm. Low-temperature experiments were performed in vapors of liquid helium ^{4}He and in a ^{3}He/^{4}He dilution cryostat. The resistance of low-resistance films with $R(T) < 1$ MΩ was measured by a standard four-probe scheme at an alternating current $I \sim 1$ nA with a low frequency $f = 3.33$ Hz. The resistance of high-resistance samples with $R(T) \geq 1$ MΩ was measured by a two-probe scheme at an ac voltage $U \sim 100$ μV with a low frequency $f = 3.33$ Hz. All measurements were performed in a linear region, which was tested by the direct measurement of the current–voltage characteristics of films.

Figure 1a shows the image of the cross section of the last superconducting film with a thickness of 10 nm in a high-resolution transmission electron microscope. The image demonstrates the deposited layers: a silicon substrate, an AlN buffer layer, and a NbTiN layer. The buffer layer was used to improve

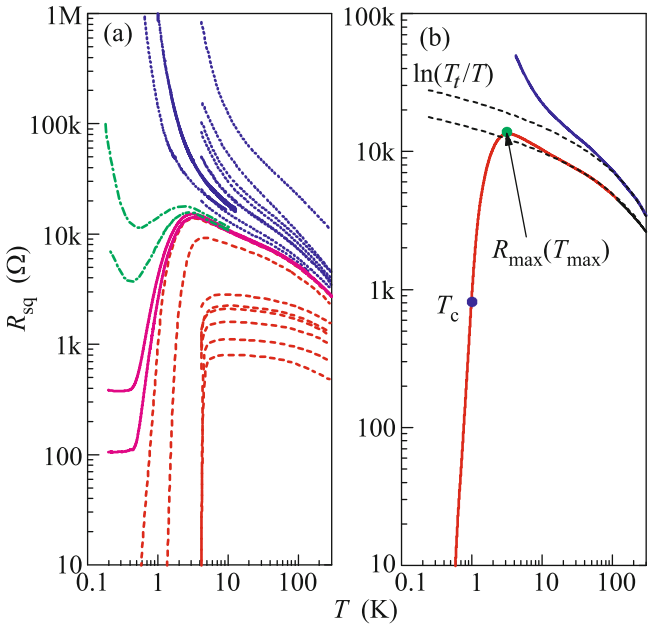

Fig. 2. (Color online) (a) Temperature dependences of the resistance of various NbTiN films on a log–log scale. (b) Illustration of the method of determination of the characteristic parameters. The solid lines are experimental data, the dashed lines correspond to the theoretical description by logarithmic law (1), and the points mark the characteristic parameters.

matching between the lattice constants of NbTiN and Si. It is seen that the film has a large degree of homogeneity in thickness and pronounced boundaries. The characteristic diffraction pattern is shown in Fig. 1b. Bright points correspond to reflections from silicon atoms in the substrate. Concentric circles characteristic of polycrystalline materials are clearly seen.

Figure 2a demonstrates the evolution of the temperature dependences of the resistance of films. The resistance of the superconducting samples with the resistance $R_{77} < 5.4$ kΩ (shown by the red dashed lines) first increases with decreasing temperature. This increase in the range $10T_c < T < 300$ K is well described by the logarithmic law

$$R(T) = R_t \ln\left(\frac{T_t}{T}\right), \qquad (1)$$

as is seen in Fig. 2b. A similar behavior of the resistance was previously observed in granular systems [21] and has not yet been completely explained [22].

With further cooling, the resistance reaches the maximum R_{max} at $T = T_{max}$ and, then, decreases to immeasurably small values, which corresponds to the transition to the superconducting state. At the same time, the resistance of films with $R_{77} > 6.2$ kΩ (shown by the blue dotted lines) increases monotonically with decreasing temperature below 0.4 K, which indicates their dielectric nature. Two samples with intermediate

R_{77} values (pink solid lines) cannot be unambiguously classified among any type because their resistance, on one hand, decreases at low temperatures and, on the other hand, does not vanish at any temperatures reached in the experiments. The resistance of the indicated films drops by an order of magnitude from R_{max} at $T < 3$ K, which indicates the formation of superconducting regions connected by weak links. It can be assumed that the quantum transport in the system in this case is determined by the relation between the effective Josephson E_J and effective Coulomb E_C components of the interaction energy of the superconducting islands. Furthermore, since the resistance of higher resistance films (shown by green dash-dotted lines) after reaching the minimum again begins to increase with decreasing temperature, it can be assumed that the energies in this case are related as $E_C > E_J$ [17].

The difference in resistance between the last superconducting and first dielectric films at 77 K is less than 2%, which indicates the disorder-induced direct superconductor–insulator transition. In addition, since the resistance of superconducting films nonmonotonically depends on the temperature, the separatrix between the superconducting and insulating sides of the transition is an inclined curve $R_{\square}(T) \neq \text{const}$, which is inconsistent with the theory [7].

The temperature dependences of the resistance of films on the superconducting side of the direct superconductor–insulator transition were analyzed with the use of the theory of quantum contributions to the conductivity [23–28] and the theory of the Berezinskii–Kosterlitz–Thouless transition [29–31]. Figure 3a shows experimental data in comparison with predictions of the theory of quantum contributions to the conductivity for some films. It is seen that good agreement between the experiment and theory is observed in the temperature range $1.5T_c < T < 20$ K. The critical temperature T_c obtained in the analysis coincides within an accuracy of 6% with the value determined from points on $R(T)$ curves at which the resistance of the film is 10% of the resistance at liquid nitrogen temperatures (the green point in Fig. 2b). The temperature T_{BKT} was determined from the approximation of experimental data by the following expression proposed in [32–34]:

$$R(T) \propto \exp\left[-b(T/T_{BKT} - 1)^{-1/2}\right]. \qquad (2)$$

Here, b is a constant about unity. The parameter T_{BKT} was chosen so that the dependences $R(T)$ are linear at temperatures $T < T_c$. The characteristic curve for one of the films is shown in Fig. 3b.

The dependences of the temperature T_c and T_{BKT} on the degree of disorder are shown in Fig. 3c. The closed symbols are experimental values of T_c and the open symbols are T_{BKT} values. The lines are the theoretical dependences of T_c on the resistance in the normal state obtained within the fermion mechanism of the suppression of superconductivity:

$$\ln\left(\frac{T_c}{T_{c0}}\right) = \frac{1}{|\gamma|} - \frac{1}{\sqrt{2r}} \ln\left(\frac{\gamma - r/4 - \sqrt{r/2}}{\gamma - r/4 + \sqrt{r/2}}\right). \qquad (3)$$

Here, $\gamma = 1/\ln(kT_{c0}\tau/\hbar)$, $r = e^2 R_{\square}(2\pi^2\hbar)^{-1}$, τ is the mean free time, and T_{c0} is the critical temperature in the bulk sample. The resistance R_{max} at the maximum of $R(T)$ and the coefficient R_t from Eq. (1) were taken as the characteristic resistance R_*. These two characteristic resistances lead to different mean free times τ.

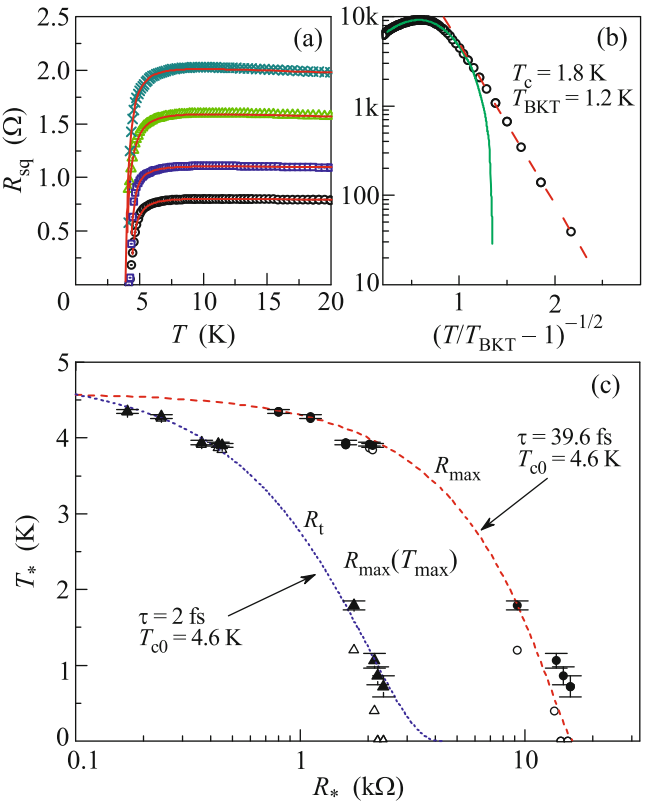

Fig. 3. (Color online) Superconducting side of the direct superconductor–insulator transition. Symbols represent experimental data. (a) Experimental points in comparison with the calculations within the theory of quantum contributions to the conductivity shown by lines. (b) Resistance of one of the films on a logarithmic scale versus the reduced temperature. The green solid line is the calculation within the theory of quantum contributions to the conductivity and the red dashed line is the approximation by Eq. (2) from [32, 33] for a vortex Berezinskii–Kosterlitz–Thouless transition. (c) (Closed symbols) Critical temperature T_c and (open symbols) Berezinskii–Kosterlitz–Thouless transition temperature T_{BKT} versus the characteristic resistance R_*. The lines are predictions within the fermion model of superconductivity suppression given by Eq. (3).

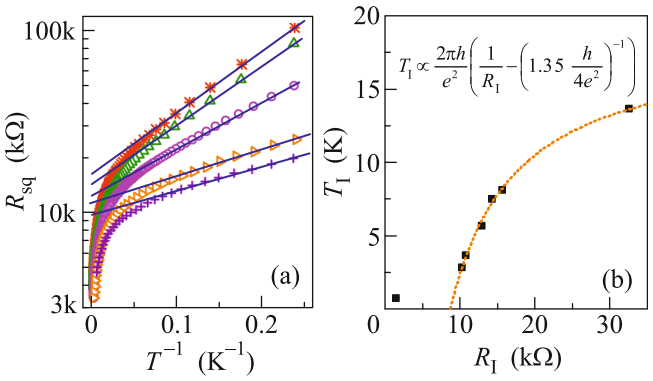

Fig. 4. (Color online) Insulating side of the direct superconductor–insulator transition. Symbols represent experimental data. (a) Resistance of films in Arrhenius coordinates. The solid straight lines correspond to the activation law (4). (b) Activation energy T_I versus the coefficient R_I. The dashed line is the empirical curve specified by Eq. (5).

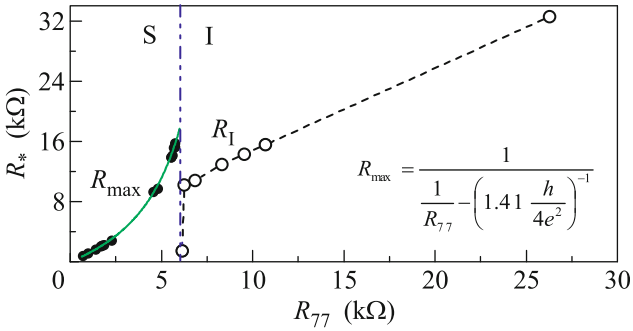

Fig. 5. (Color online) Resistance at the maximum R_{max} and the coefficient R_I versus the degree of disorder. The solid line is the empirical curve specified by Eq. (6) and the dash-dotted line is the boundary of the superconductor–insulator transition.

The τ value corresponding to the curve $T_*(R_t)$ is closer to the mean free time determined in the mean field approximation. Any other choice of the characteristic resistance results in the dependence $T_*(R_*)$ lying between the mentioned curves. In this case, discrepancy of experimental data and fermion model results for $R_* = R_{max}$ is observed: the critical temperature is suppressed much more slowly than the theoretically predicted value.

The choice of R_t as the characteristic resistance makes it possible to reach the best agreement between experimental data and predictions of the fermion model of the suppression of superconductivity. The temperature of the Berezinskii–Kosterlitz–Thouless transition vanishes at a nonzero critical temperature, which is characteristic of the boson model. Thus, the boson and fermion mechanisms of the suppression of superconductivity are simultaneously implemented in the studied system.

Further, we consider films on the insulating side of the direct superconductor–insulator transition. The resistance curves for them were represented in activation coordinates (see Fig. 4a). At temperatures below 10 K, good agreement is observed with the Arrhenius law characteristic of insulators:

$$R(T) = R_I \exp\left(\frac{T_I}{T}\right). \qquad (4)$$

The activation energy $E_I = k_B T_I$ increases monotonically with disorder from 0.24 to 2.07 meV in agreement with experimental results obtained for TiN thin films [15]. The dependence of T_I on the prefactor R_I (Fig. 4b) is hyperbolic:

$$T_I \propto \frac{2\pi h}{e^2}\left(\frac{1}{R_I} - \frac{1}{R_{trI}}\right), \qquad (5)$$

where $R_{trI} = 1.35(h/4e^2)$ is about the resistance quantum $h/4e^2$ for Cooper pairs, which corresponds to the critical resistance R_c in the boson model. The resistance R_{trI} corresponds to the resistance $R_{77} = 1.1(h/4e^2)$, which is slightly above the threshold value $R_{SI} = 6$ kΩ of the resistance of the superconductor–insulator transition in studied films. Moreover, the activation energy of the lowest resistance insulators, which have a nonmonotonic dependence $R(T)$, is beyond the line specified by Eq. (5), which is apparently due to the strong inhomogeneity of the transport properties, which appears at the superconductor–insulator transition.

The resistance R_{max} (closed symbols in Fig. 5) and the coefficient R_I (open symbols in Fig. 5) increase with the degree of disorder. The R_I value for insulating films near the direct superconductor–insulator transition is much smaller than the R_{max} value for superconducting films. The dependence of R_I in these coordinates is close to linear except for R_I values of the lowest resistance insulators, which have a nonmonotonic dependence $R(T)$. Meanwhile, the resistance R_{max} has the hyperbolic dependence

$$R_{max} = \frac{1}{R_{77}^{-1} - R_{trS}^{-1}}, \qquad (6)$$

where $R_{trS} = 1.41(h/4e^2)$ is also about the resistance quantum for Cooper pairs but is much larger than the threshold resistance of the superconductor–insulator transition R_{SI}.

To summarize, an increase in the resistance in the normal state, which is due to a decrease in the thickness of films, results in the shift of the maximum resistance toward lower temperatures from 10.6 to 3.1 K, a monotonic decrease in the critical temperature of the superconducting transition from 4.35 to 0.72 K, the

complete suppression of T_{BKT} for films on the superconducting side of the direct superconductor–insulator transition, and an increase in the activation energy and the coefficient R_I for films on the insulating side of the direct superconductor–insulator transition.

The studies of the low-temperature transport were supported by the Council of the President of the Russian Federation for Support of Young Scientists and Leading Scientific Schools (project no. MK-4628.2016.2). The studies of the structure of NbTiN films were supported by the Russian Science Foundation (project no. 14-22-00143). The fabrication of the films (T.P.) and the interpretation of the data (V.M.V.) were supported by the US Department of Energy, Office of Science, Basic Energy Sciences, Materials Sciences and Engineering Division.

REFERENCES

1. A. I. Shal'nikov, Nature (London) **142**, 74 (1938).
2. A. M. Goldman and N. Marković, Phys. Today **51** (11), 39 (1998).
3. V. F. Gantmakher and V. T. Dolgopolov, Phys. Usp. **53**, 1 (2010).
4. M. Strongin, R. S. Thompson, O. F. Kammerer, and J. E. Crow, Phys. Rev. B **1**, 1078 (1970).
5. A. M. Finkel'shtein, Sov. Phys. JETP **59**, 212 (1984).
6. A. Gold, Phys. Rev. A **33**, 652 (1986).
7. M. P. A. Fisher, G. Grinstein, and S. Grivin, Phys. Rev. Lett. **64**, 587 (1990).
8. J. M. Graybeal and M. R. Beasley, Phys. Rev. B **29**, 4167 (1984).
9. A. Yazdani and A. Kapitulnik, Phys. Rev. Lett. **74**, 3037 (1995).
10. S. Okuma, T. Terashima, and N. Kokubo, Phys. Rev. B **58**, 2816 (1998).
11. A. F. Hebard and M. A. Paalanen, Phys. Rev. Lett. **65**, 927 (1990).
12. D. Shahar, Z. Ovadyahu, and A. M. Goldman, Phys. Rev. B **46**, 10917 (1992).
13. V. Gantmakher, M. V. Golubkov, V. T. Dolgopolov, G. E. Tsydynzhapov, and A. A. Shashkin, Physica B **284–288,** 649 (2000).
14. E. Bielejec, J. Ruan, and W. Wu, Phys. Rev. B **63**, 100502 (2001).
15. T. I. Baturina, A. Yu. Mironov, V. M. Vinokur, M. R. Baklanov, and C. Strunk, Phys. Rev. Lett. **99**, 257003 (2007).
16. M. V. Feigelman, L. B. Ioffe, V. E. Kravtsov, and E. Cuevas, Ann. Phys. **325**, 1390 (2010).
17. T. I. Baturina and V. M. Vinokur, Ann. Phys. **331**, 236 (2013).
18. J. R. Gavaler, M. A. Janocko, A. Patterson, and C. K. Jones, J. Appl. Phys. **42**, 54 (1971).
19. J. Jesudasan, M. Mondal, M. Chand, A. Kamlapure, S. Kumar, G. Saraswat, V. C. Bagwe, V. Tripathi, and P. Raychaudhuri, AIP Conf. Proc. **1349**, 923 (2011).
20. M. Mondal, A. Kamlapure, M. Chand, G. Saraswat, S. Kumar, J. Jesudasan, L. Benfatto, V. Tripathi, and P. Raychaudhuri, Phys. Rev. Lett. **106**, 047001 (2011).
21. R. W. Simon, B. J. Dalrymple, D. Van Vechten, W. W. Fuller, and S. A. Wolf, Phys. Rev. B **36**, 1962 (1987).
22. I. S. Beloborodov, A. V. Lopatin, V. M. Vinokur, and K. B. Efetov, Rev. Mod. Phys. **79**, 469 (2007).
23. L. G. Aslamasov and A. I. Larkin, Phys. Lett. A **26**, 238 (1968).
24. K. Maki, Prog. Theor. Phys. **39**, 897 (1968).
25. R. S. Thompson, Phys. Rev. B **39**, 327 (1970).
26. S. Hikami, A. I. Larkin, and Y. Nagaoka, Prog. Theor. Phys. **63**, 707 (1980).
27. B. L. Altshuler, A. G. Aronov, and P. A. Lee, Phys. Rev. Lett. **44**, 1288 (1980).
28. B. L. Al'tshuler, A. A. Varlamov, and M. Yu. Reizer, Sov. Phys. JETP **57**, 1329 (1983).
29. V. L. Berezinskii, Sov. Phys. JETP **34**, 610 (1971).
30. J. M. Kosterlitz and D. J. Thouless, J. Phys. C: Solid State Phys. **6**, 1181 (1973).
31. J. M. Kosterlitz, J. Phys. C: Solid State Phys. **7**, 1046 (1974).
32. B. I. Halperin and D. R. Nelson, J. Low Temp. Phys. **36**, 599 (1979).
33. S. Doniach and B. A. Huberman, Phys. Rev. Lett. **42**, 1169 (1979).
34. M. J. Buckingham and W. M. Fairbank, Prog. Low Temp. Phys. **3**, 80 (1961).